JOURNAL OF Materials CHEMISTRY

Microstructure and electron transport properties of Au_xCo_{1-x} nano-alloys embedded in polyacrylonitrile thin films

Hideki Nabika, Kensuke Akamatsu,† Minoru Mizuhata, Akihiko Kajinami and Shigehito Deki*

Department of Chemical Science and Engineering, Faculty of Engineering, Graduate School of Science & Technology, Kobe University, Rokkodai, Nada, Kobe, 657-8501, Japan. E-mail: deki@kobe-u.ac.jp

Received 12th April 2002, Accepted 14th May 2002
First published as an Advance Article on the web 14th June 2002

Au_xCo_{1-x} nano-alloys with a diameter below 10 nm were fabricated *via* a vacuum co-evaporation method. The composition dependence and the effect of heat-treatment on the microstructure of the Au_xCo_{1-x} nano-alloys were investigated by means of electron diffraction analysis. The lattice constant of fcc Au_xCo_{1-x} nano-alloys varied with the composition and heat-treatment. The results revealed that as-deposited Au_xCo_{1-x} nano-alloys were in a thermodynamically metastable state, and the following heat-treatment led to their equilibrium state. Furthermore, phase transition from fcc solid solution to $L1_0$-type ordered face-centered tetragonal (fct)-structure partially took place during heat-treatment. The temperature and magnetic field dependences of electrical resistivity were investigated for polyacrylonitrile (PAN) thin films embedded with Au_xCo_{1-x} nano-alloys, and a TMR value of 80% was obtained at room temperature under appropriate conditions.

Introduction

Nano-sized bimetallic colloids or clusters are of great interest from both scientific and technological viewpoints, because of their potential to exhibit novel properties which cannot be achieved by monometallic nanoparticles. Much effort has been devoted for the fabrication of several types of nano-alloys in order to improve the performance of catalytic materials such as electrocatalysts[1–4] and catalysts for chemical reactions.[5–8] Magnetic nano-alloys consisting of ferromagnetic elements are also investigated for the purpose of anomalous magnetic properties, for instance, magnetoresistance (MR).[9–14] Various types of MR materials are widely utilized in advanced technology such as read heads for high-density magnetic storage. Tunneling magnetoresistance (TMR) is one of the MR phenomena originating from spin-dependent tunneling of electrons among neighboring magnetic particles, which was first investigated by Gittleman *et al.* for Ni–SiO_2 films.[15]

One of the most interesting features for these nanoscopic materials, including monometallic nanoparticles and bimetallic nano-alloys, is the difference in the thermodynamical properties (melting point or mutual solubility) compared to the bulk materials. It is well known that the melting point of monometallic nanoparticles decreases with the decrease of their size down to the nanometer scale.[16,17] Yasuda *et al.* have studied the "spontaneous alloying", in which extremely rapid dissolution of solute atoms into nanoparticles takes place when solute atoms are vapour deposited onto nano-sized clusters,[18–20] as well the stability of alloy phases for nanoscopic materials.[21,22] According to their results, it seems that novel nano-alloys which could not detected in the bulk phase diagrams can be observed, and further investigations are required for the development of novel nanoscopic materials in various fields.

In our previous study,[23] we have reported on carbon thin films containing Au_xCo_{1-x} nano-alloys, prepared by heating polyacrylonitrile (PAN) thin films deposited with Au_xCo_{1-x} nano-alloys through co-evaporation of Au and Co. We found that Au_xCo_{1-x} nano-alloys dispersed into PAN matrix after heat-treatment at 200 °C, and we finally obtained carbon thin films containing Au_xCo_{1-x} nano-alloys upon heating at 600 °C owing to carbonization of the PAN matrix. It should be noted here that the Au/Co binary system is a typical phase separated system in the corresponding phase diagram.[24] In the present study, we concentrated on the microstructural investigation of Au_xCo_{1-x} nano-alloys, especially on the composition dependence and the effects of heat-treatment. Crystal structure and lattice parameter were determined by the means of selected area electron diffraction (SAED) analysis. We also describe our investigation on the temperature and the magnetic field dependences of electron transport properties of PAN thin films embedded with Au_xCo_{1-x} nano-alloys.

Experimental procedure

A glass vacuum chamber was first evacuated down to 2.0×10^{-5} Torr, and PAN (Aldrich) with the thickness of 50 nm was vapour deposited onto the substrates using a resistance-heated molybdenum boat. Au and Co metals were then co-deposited onto the PAN layer using two independent alumina-coated tungsten filaments, and then a PAN layer (50 nm) was again deposited. The purities were 99.99% for Au and 99.8% for Co, respectively. The amount and the rate of deposition were monitored using a quartz crystal microbalance (QCM). During metal deposition, two independent QCMs were used. The total metal concentration in the metal/PAN composite film was kept constant at 5 vol% for each composition. After the deposition, samples were heat-treated under nitrogen flow in the temperature range 100–600 °C for 1 h.

For the structural investigation of the co-deposited nano-alloys, a JEM-2010 (JEOL) transmission electron microscope (TEM) equipped with an energy dispersive X-ray spectrometer (EDX, NORAN Instrument, Inc.) was used. The operation was carried out with an accelerating voltage of 200 kV. The temperature dependence of the resistivity was measured in the range 300–75 K with a closed cycle He cryostat (Optistat CF1204, Oxford). Applied magnetic field dependence of the

†Present address: Department of Chemistry, Faculty of Science and Engineering, Konan University, Okamoto, Higashinada, Kobe 658-8501, Japan.

 DOI: 10.1039/b203600b

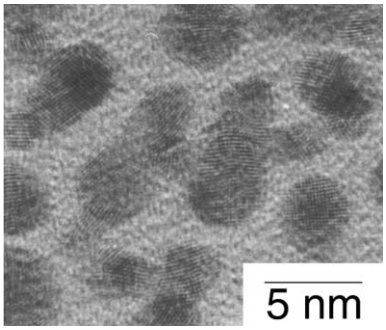

Fig. 1 Typical TEM image of co-deposited $Au_{0.5}Co_{0.5}$ nano-alloy.

resistivity was measured up to 1.1 T. The magnetic field was applied in the film plane parallel to the current direction.

Results and discussion

Microstructure of Au_xCo_{1-x} nano-alloys

Fig. 1 shows a typical TEM image of Au–Co co-deposited nanoparticles ($Au_{0.5}Co_{0.5}$), in which nanoparticles with an average diameter approximately 3 nm and clear lattice fringes are observed. X-Ray photoelectron spectroscopy and EDX analysis (not shown here) confirmed that the obtained nanoparticles observed in Fig. 1 were not monometallic Au or Co nanoparticles, but bimetallic Au/Co nano-alloys. To investigate the crystal structure of Au_xCo_{1-x} nano-alloys in detail, an SAED study was employed. SAED patterns obtained were calibrated by using the *d*-spacing of single crystalline Au thin film. Fig. 2 shows SAED patterns of as-deposited samples with different composition, in which the SAED pattern of the reference sample deposited with only Au is also shown. The reference sample shows a typical diffraction pattern of fcc structure with a lattice spacing of 4.06 Å (Table 1). It can be clearly seen that each diffraction peak broadens with increasing Co content. For the as-deposited sample, the lattice parameters obtained from SAED patterns are found to be relatively close to that of bulk Au (Table 1). Tsaur *et al.* pointed out that the addition of small amounts of Au to Co (even a few atom%)

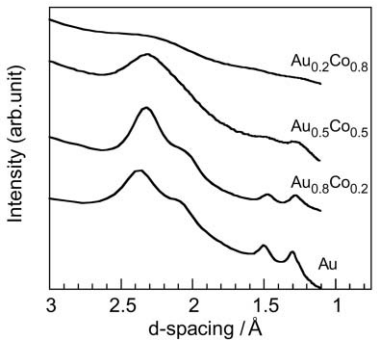

Fig. 2 Changes in the SAED patterns with respect to the composition of Au/Co.

Table 1 Lattice parameters of Au_xCo_{1-x} nano-alloys before and after heat-treatment at 600 °C. Calculated values based on the Vegard's law are also shown

	Lattice parameter/Å		
Composition	as-dep.	600 °C	Vegard's law
Au	4.06	4.07	4.079
$Au_{0.8}Co_{0.2}$	4.02	3.97	3.972
$Au_{0.5}Co_{0.5}$	4.02	3.78	3.813
$Au_{0.2}Co_{0.8}$	3.96	3.70	3.652
Co	—	—	3.545

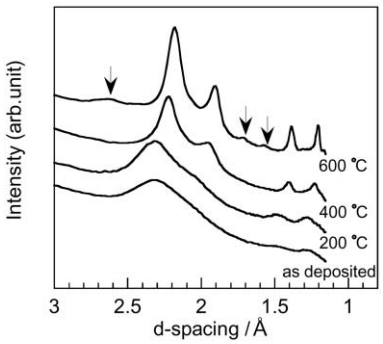

Fig. 3 Variation of the SAED patterns for the $Au_{0.5}Co_{0.5}$ nano-alloy with heat-treatment.

could affect the crystal structure and the resulting alloys favor the crystal structure of Au.[25] Especially for the present study, this effect seems to be pronounced because Au_xCo_{1-x} nano-alloys have been prepared by vacuum evaporation, which is a quenching method. As a result, it is suggested that the obtained Au_xCo_{1-x} nano-alloys are in thermodynamically metastable state, and their crystal structure is close to that of Au even at Co contents up to 80%.

Fig. 3 shows the variation of the SAED patterns of $Au_{0.5}Co_{0.5}$ nano-alloys with heat-treatment up to 600 °C. The diffraction position and intensity do not show any significant changes up to 200 °C, whereas each diffraction peak becomes sharper and shifts towards lower *d*-spacing values with increasing heat-treatment temperature above 400 °C. The lattice parameter after the heat-treatment at 600 °C, 3.78 Å (Table 1), is no longer close to that of Au. Instead this value is rather close to the calculated value, 3.813 Å, based on Vegard's law for an Au/Co solid solution with an atomic ratio of 1 : 1. In this calculation, the lattice parameter of fcc-Co, rather than hcp-Co, was used, since the fcc phase is more energetically favored than the hcp phase when the particle diameter is below 20 nm.[26] This behavior was observed for all the samples with different compositions. After the heat-treatment at 600 °C, some weak diffraction peaks assigned to an $L1_0$-type ordered structure are also observed (indicated with arrows in Fig. 3), whereas there are no diffraction lines from monometallic Au or Co. SAED studies reveal that the as-deposited Au_xCo_{1-x} nano-alloys obtained in the present study are thermodynamically metastable, and the following heat-treatment releases the internal stress and leads to their equilibrium state, resulting in the changes of the lattice parameter.

Electron transport properties

The temperature dependence of the electrical resistivity ρ of PAN thin films containing $Au_{0.2}Co_{0.8}$ nano-alloys heat-treated at various temperatures are plotted in Fig. 4. The electrical resistivity shows good linear correlation with $T^{-1/2}$ for all the samples. This is a typical relation for electron tunneling conduction for insulating materials containing metal nanoparticles,[27–29] which was previously explained by Sheng *et al.*[27] taking into account both temperature-dependent and temperature-independent components of the tunneling probability. They calculated the electrical resistivity and obtained the final formula as:

$$\log\rho = 2(C/k_B)^{1/2}T^{-1/2} + \text{const.} \quad (1)$$

where $C = ((2\pi/h)(2m\varphi)^{1/2}sE_c)$ is the activation energy for electron tunneling. k_B, T, h and m are Boltzmann constant, absolute temperature, Planck's constant and effective electron mass, respectively; φ, s and E_c represent effective barrier height, barrier width and Coulomb energy, respectively. From the gradient of log ρ *vs.* $T^{-1/2}$ shown in Fig. 4, the activation energy, C, is estimated to be 0.51 eV for the as-deposited

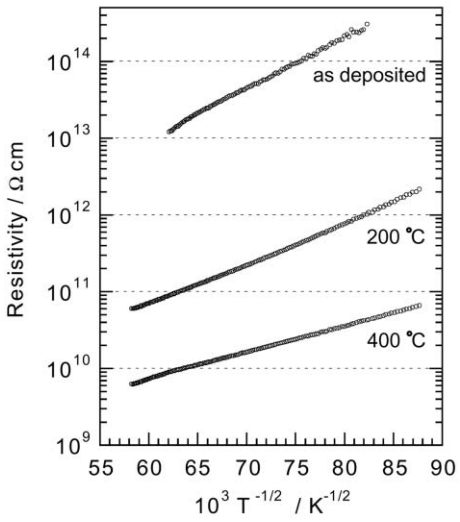

Fig. 4 Temperature dependence of electrical resistivity of PAN thin films containing $Au_{0.5}Co_{0.5}$ nano-alloys before and after heat-treatment.

sample and 0.13 eV after heat-treatment at 400 °C. The dominant factors for the decrease of C upon heat-treatment is thought to be the lowering of the barrier height of the matrix owing to carbonization and the reduction of Coulomb energy because of particle growth (about 8 nm after the heat-treatment at 400 °C).

Fig. 5 shows the magnetic field dependence of the electrical resistivity for as-deposited samples. Here, the MR ratio, $\Delta\rho/\rho_0$, is defined as follows,

$$\Delta\rho/\rho_0 = \frac{\rho(\mu_0 H) - \rho(\mu_0 H = 0)}{\rho(\mu_0 H = 0)} \times 100 \quad (2)$$

The origin of TMR is *via* spin-dependent tunneling of electrons between two magnetic particles, for which the tunneling probability changes with the relative angle between magnetization vectors of the nearest neighbor particles. The relative angle, which changes according to the applied field, is closely related to the relative magnetization. The relation between the MR ratio and relative magnetization is expressed as follows:

$$\text{MR ratio} \propto (M/M_S)^2 \quad (3)$$

where M is global magnetization and M_s the saturation magnetization. Assuming that the samples are in a superparamagnetic state, the magnetization can be expressed by using a Langevin function; $L(x) = \coth(x) - 1/x$. If the number of magnetic particles with magnetic moment m is N in a unit volume, magnetization can be expressed by using Langevin function L(x) as:

$$M = NmL(mH/k_B T) \quad (4)$$

$$M_S = NmL(mH_S/k_B T) \quad (5)$$

Here H_s is the applied magnetic field where all of the magnetic vectors arrange in a parallel manner. Solid lines in Fig. 5 represent the fitting data calculated based on the equations (3)–(5). We obtained an MR ratio of about 80% for $Au_{0.2}Co_{0.8}$ at room temperature. On the other hand, only slight changes were observed for $Au_{0.5}Co_{0.5}$, and plots for the $Au_{0.8}Co_{0.2}$ nano-alloys showed no dependence with applied field, because of the dilution of the magnetic moment.[30]

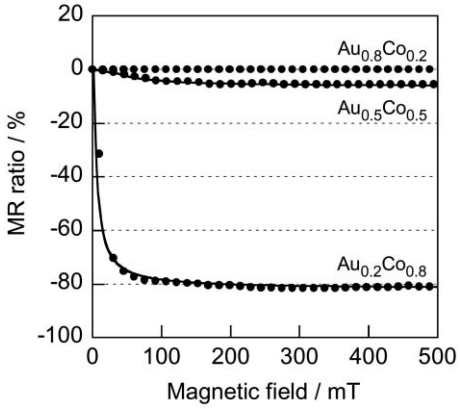

Fig. 5 Composition dependence of the MR curves of PAN thin films containing Au/Co nano-alloys.

Conclusion

SAED analysis has been used for microstructural characterization of Au_xCo_{1-x} nano-alloys obtained *via* the vacuum co-evaporation method. Fcc structures were found for as-deposited Au_xCo_{1-x} nano-alloys and their lattice constants were relatively close to that of bulk Au even up to a Co content of 80%. Although as-deposited Au_xCo_{1-x} nano-alloys were thermodynamically metastable, especially for high Co content, heat-treatment at 600 °C released the internal stress and led to the equilibrium states, in which the lattice constants of the resulting Au_xCo_{1-x} nano-alloys obeyed Vegard's law. It was also noticed that $L1_0$-type ordered-structure was partially obtained after the heat-treatment at 600 °C. From the results of temperature and magnetic field dependences of electrical resistivity, it was found that PAN thin films embedded with Au_xCo_{1-x} nano-alloys showed electron tunneling conduction, with the tunneling probability varying with magnetic field. The maximum TMR value obtained in the present study was *ca.* 80% for $Au_{0.2}Co_{0.8}$ system at room temperature.

Acknowledgement

A part of this study has been supported by CREST of JST (Japan Science and Technology) and Grant-in-aid for Scientific Research No.13875127 from the Ministry of Education, Science, Sports, and Culture, Japan.

References

1 H. A. Gasteiger, N. Markovic, P. N. Ross Jr and E. J. Cairns, *J. Phys. Chem.*, 1994, **98**, 617.
2 R. Ianniello, V. M. Schmidt, J. L. Rodriguez and E. Pastor, *J. Electroanal. Chem.*, 1999, **471**, 167.
3 L. J. Wan, T. Moriyama, M. Ito, H. Uchida and M. Watanabe, *Chem. Commun.*, 2002, 58.
4 H. Igarashi, T. Fujino, Y. M. Zhu, H. Uchida and M. Watanabe, *Phys. Chem. Chem. Phys.*, 2001, **3**, 306.
5 N. Toshima and T. Yonezawa, *New J. Chem.*, 1998, 1179.
6 P. Lu, T. Teranishi, K. Asakura, M. Miyake and N. Toshima, *J. Phys. Chem. B.*, 1999, **103**, 9673.
7 Y. Mizukoshi, T. Fujimoto, Y. Nagata, R. Oshima and Y. Maeda, *J. Phys. Chem. B.*, 2000, **104**, 6028.
8 L. Guczi, L. Borko, Z. Schay, D. Bazin and F. Mizukami, *Catal. Today*, 2001, **65**, 51.
9 G. N. Kakazei, A. F. Kravetz, N. A. Lesnik, M. M. Pereira de Azevedo, Yu. G. Pogorelov, G. V. Bondarkova, V. I. Silantiev and J. B. Sousa, *J. Magn. Magn. Mater.*, 1999, **197**, 29.
10 L. Xi, Z. Z. Zhang, J. H. Chi, C. X. Li and S. H. Ge, *Chin. Sci. Bull.*, 2001, **46**, 734.
11 K. Inomata and Y. Saito, *J. Magn. Magn. Mater.*, 1999, **199**, 18.
12 K. Inomata and Y. Saito, *Appl. Phys. Lett.*, 1998, **73**, 1143.
13 Y. Saito, K. Nakajima, K. Tanaka and K. Inomata, *IEEE Trans. Magn.*, 1999, **35**, 2904.
14 X. F. Han *et al.*, *Appl. Phys. Lett.*, 2000, **77**, 283.
15 J. L. Gittleman, Y. Goldstein and S. Bozowski, *Phys. Rev. B*, 1972, **5**, 3609.
16 P. Buffat and J. P. Borel, *Phys. Rev. A*, 1976, **13**, 2287.
17 T. Castro, R. Reifenberger, E. Choi and R. P. Andres, *Phys. Rev. B*, 1990, **42**, 8548.

18 H. Yasuda, H. Mori, M. Komatsu and K. Takeda, *J. Appl. Phys.*, 1993, **73**, 1100.
19 H. Yasuda and H. Mori, *Mater. Sci. Eng. A*, 1996, **217/218**, 249.
20 H. Yasuda and H. Mori, *Thin Solid films*, 1997, **298**, 143.
21 H. Mori and H. Yasuda, *Mater. Sci. Eng. A*, 1996, **217/218**, 244.
22 H. Yasuda, K. Mitsuishi and H. Mori, *Phys. Rev. B*, 2001, **64**, 094101.
23 S. Deki, H. Nabika, K. Akamatsu, M. Mizuhata and A. Kajinami, *Scr. Mater.*, 2001, **44**, 1879.
24 *Phase Diagrams of Binary Gold Alloys*, ed. H. Okamoto and T. B. Massalski, ASM International, T. M. Metals Park, Ohio, 1987.
25 B. Y. Tsaur, S. S. Lau and J. W. Mayer, *Philos. Mag. B*, 1981, **44**, 95.
26 O. Kitakami, H. Sato, Y. Shimada, F. Sato and M. Tanaka, *Phys. Rev. B*, 1997, **56**, 13849.
27 P. Sheng, B. Abeles and Y. Arie, *Phys. Rev. Lett.*, 1973, **31**, 44.
28 J. S. Helman and B. Abeles, *Phys. Rev. Lett.*, 1976, **37**, 1429.
29 P. Sheng and J. Klfter, *Phys. Rev. B*, 1983, **27**, 2583.
30 T. R. McGuire, J. A. Aboaf and E. Klokholm, *J. Appl. Phys.*, 1981, **52**, 2205.